UDC 528.72:621.391.822 **doi: 10.32620/reks.2025.2.09**

Viktoriia NAUMENKO, Volodymyr LUKIN, Vitalii NAUMENKO,
Nadiia KOZHEMIAKINA, Mykyta SOLODOVNYK

National Aerospace University "Kharkiv Aviation Institute", Kharkiv, Ukraine

COMPARATIVE ANALYSIS OF THE EFFECTIVENESS OF BPG, AGU, AVIF AND HEIF COMPRESSION METHODS FOR MEDICAL IMAGES CORRUPTED BY NOISE OF TWO TYPES

*The **subject** matter is lossy compression using the BPG, AGU, AVIF, and HEIF encoders for medical images with different levels of visual complexity corrupted by additive Gaussian and Poisson noise. The **goal** of this study is to compare encoders regarding optimal image compression parameters and select the most suitable metric to determine the optimal operation point. The **tasks** considered include: selecting 512x512 grayscale test images with various degrees of visual complexity, including visually complex images rich in edges and textures, moderately complex images with edges and textures adjacent to homogeneous areas, and visually simple images consisting mainly of homogeneous areas; establishing image quality assessment metrics and evaluating their effectiveness under different encoder compression parameters; selecting one or more metrics that clearly determine the position of the optimal operation point; providing recommendations based on the results obtained for compressing medical images corrupted by additive white Gaussian and Poisson noises using four encoders to maximize the quality of the restored image to the noise-free original. The employed **methods** encompass image quality assessment techniques employing MSE, PSNR, and MSSIM metrics, as well as software modeling in Python without using the built-in Poisson noise generator. The **results** show that optimal operation points (OOPs) can be determined for all these metrics when the quality of the compressed image is better than the quality of the corresponding noisy original image, accompanied by a sufficiently high compression ratio. Moreover, achieving an appropriate balance between the compression ratio and image quality leads to partial noise reduction without noticeable information content distortion in the compressed image. This study emphasizes the importance of using appropriate metrics to assess the quality of compressed medical images and provides insight into the determination of the compression parameter Q to achieve the optimal operation point of the BPG encoder for specific images. However, the position of the OOP and its presence depend not only on the image complexity but also on the chosen encoder. **Conclusions.** The scientific novelty of the obtained results includes: 1) The consideration of noise models and parameter levels typical for medical imaging, namely, additive Gaussian noise of such intensity that it approximately corresponds to just noticeable differences, and signal-dependent Poisson noise; 2) The analysis of the multi-scale structural similarity index (MS-SSIM), which has not been previously explored in studies on lossy compression of noisy medical images; 3) A detailed examination of AVIF and HEIF coders to determine whether the optimal operating point (OOP) is observed for them and under which noise conditions; 4) The use of a dataset comprising ten medical images of varying visual complexity, with generalized tendencies revealed for different structural types; 5) The identification of the ability of many metrics to exhibit an OOP for images of moderate visual complexity or those dominated by homogeneous areas; 6) For Poisson noise, the demonstration of a dependence between the quality factor Q in the OOP and the average image intensity, which can be practically estimated for a given image; 7) The finding that different encoders require different approaches to determine their respective OOPs due to their distinct compression control parameters; 8) The observation that compression ratios achieved at the OOP are generally high, supporting the feasibility of using the OOP or its neighbourhood in practice.*

***Keywords:** lossy image compression; BPG; AGU; AVIF; HEIF; AWGN; Poisson noise; optimal operation point.*

1. Introduction

Medical image compression is of great importance in the healthcare industry because it can significantly increase the efficiency of data transmission and storage and reduce the costs associated with medical imaging. With the proliferation of digital technologies in diagnostics and treatment, the volume of medical images has grown significantly, creating problems with their storage, transmission, and processing [1]. Efficient image transmission, particularly in constrained environments such as Wireless Multimedia Sensor Networks (WMSN), has become a critical task, prompting research into advanced methods, including those based on the Residue Number System [2, 3]. Medical image compression technologies can help solve these problems by reducing the need for

ISSN 1814-4225 (print)
ISSN 2663-2012 (online)

data storage and transmission without losing the image diagnostic quality [4, 5]. This contributes to faster and more reliable diagnoses, reduced storage and transmission costs, and improved care quality. Medical image compression is extremely important for telemedicine and remote medical services, where efficient image transmission is critical for timely diagnosis and treatment.

1.1. Motivation

Two types of compression are commonly used in digital image processing: lossless compression and lossy compression [6]. Lossless compression, as the name implies, allows one to fully restore a compressed image to its original state without any data loss. This approach is often used in medical imaging, where even the slightest loss of information can significantly affect diagnosis and treatment decisions [7, 8]. In contrast to lossless compression, lossy compression [9, 10] involves removing some data from the image to achieve a higher compression ratio. Although this approach can significantly reduce the file size, it also leads to a certain loss of image quality, which may be unacceptable in medical imaging [11, 12].

The compression of medical images requires consideration of some special requirements. First, the diagnostic quality of the compressed images must be preserved so that they remain as informative as the original. In addition, the compression process must ensure fast and efficient image transfer and storage while meeting the healthcare industry's security and privacy requirements. Compatibility of compressed images with various software and medical equipment used in clinical practice is another important condition. Fulfilling these requirements is critical for the effective use of compressed images in medical practice [13, 14].

However, these are not the only problems encountered. Noise present in the collected images can significantly affect their quality, as it obscures important areas and details.

Medical imaging systems, such as X-ray machines and computed tomography (CT) scanners, create images of a patient's body area using X-rays or CT scans, recording the degree of absorption [15].

Noise in such images is often modelled using a Poisson distribution and is known as Poisson noise, shot noise, photon noise, Schott noise, or quantum noise. The peculiarity of Poisson noise is peculiar in that it does not depend on temperature or frequency but is caused by the process of counting photons. Its intensity is directly proportional to the brightness of the pixels: pixels with higher brightness have a greater noise variance than those with darker brightness [16].

In addition to Poisson noise, additive white Gaussian noise (AWGN), which arises from various electronic factors in data acquisition and transmission systems, is also often present in medical images [17]. This noise is evenly distributed throughout the image and can further degrade image quality, making it difficult to detect subtle structures or pathological changes.

Although neural network-based methods for compression and denoising are increasingly being studied, this study focuses on standardized codecs currently adopted in practical healthcare systems.

1.2. State of the art

In the presence of noise, image compression requires a special approach. Lossless compression is especially sensitive to noise because its efficiency is significantly reduced, and the compression ratio (CR) can be very close to unity [18]. In this regard, using lossy compression, which provides higher CR values and has a number of additional advantages, is advisable.

One of these advantages is the effect of noise filtering, which is achieved by adjusting certain parameters accordingly. This effect was first discovered in [19] and is observed when various orthogonal transformations are applied in compression methods [12, 18, 19]. This noise-suppressing property can be enhanced by integrating learnable denoising blocks into the compression pipeline [20].

The coding parameters must be chosen so that compression occurs near the optimal operation point (OOP) [21, 22], which ensures the maximum similarity of the decoded image to the noise-free original according to a given criterion. Meanwhile, medical images have not been studied in [21, 22]. In addition, we consider the noise characteristics more typical for medical images that were not analyzed in [21, 22].

In deep learning-based compression systems, the OOP can be learned directly from data using perceptual and structural loss functions [23].The possible existence of the OOP has been confirmed for various types of noise [19], as well as for compression methods based on the discrete cosine transform (DCT) [24, 25] and wavelets [26]. OOP can be determined using criteria such as mean squared error (MSE), peak signal-to-noise ratio (PSNR) [27, 28], and visual quality metrics such as PSNR-HVS-M and MSSIM [29]. Modern metrics, such as LPIPS or NIQE, have been proposed to better reflect human perception, especially in the presence of noise [30].

However, it remains challenging to automatically provide compression near the OOP with complex types of signal-dependent noise. Several recent works have proposed adaptive compression schemes where parameters are dynamically tuned based on local noise statistics [31]. These developments demonstrate a shift toward image coding techniques that are context- and noise-aware.

1.3. Objectives and tasks

The relevance of studying the effect of these types of noise on the efficiency of lossy compression has increased, especially in the field of medical imaging, where various noise distortions influence the formation of images. In this study, we consider the lossy compression properties of images corrupted with additive Gaussian and Poisson noise. The analysis is carried out for four modern encoders: BPG [32], AGU [33], AVIF, and HEIF [34], and recommendations for choosing compression parameters for noisy images are provided.

To achieve the goal, within the framework of this publication, the following tasks must be solved:

1. The dependence of the MSE metric for noisy medical images with additive white Gaussian noise (AWGN) and Poisson noise was analyzed using different coders (BPG, AGU, AVIF, HEIF).
2. Determine the optimal values of the Q parameter that provide minimal image distortion for each coder and noise type according to the MSE, PSNR, and MSSIM metrics.
3. Compare the results of different encoders by quality metrics at optimal operating points (OOP).
4. The compression efficiency at optimal operating points for each encoder was evaluated in terms of preserving the required image quality and the amount of memory saved.
5. Analyze the suitability of encoders for automatic application in medical systems, considering the stability of the behavior metric and the predictability of the position of the optimal operating point Q. To identify the limitations and prospects for further research, particularly for the less studied AVIF and HEIF encoders.

The article is organized as follows:

Section 2 describes the research methods, including subsections: 2.1. Noise models, 2.2. Image model, 2.3. Techniques for Controlling the Efficiency of Lossy Compression and 2.4. Considered compression methods.

Section 3 presents the results: the optimal compression parameters for four encoders (BPG, AGU, AVIF, HEIF) are determined, and a comparison is made in terms of quality metrics and compression ratio.

Conclusions and recommendations for the practical use of compression in medical systems are presented in Section 4.

2. Materials and research methods

When evaluating image compression methods for noisy images, both the image and noise models must be considered. To understand the impact of noise on the compression process, its statistical characteristics must be clearly defined. In this article, we consider two types of the noise: additive white Gaussian noise (AWGN) and Poisson noise. Signal-dependent noise might have a completely different effect on compression than signal-independent noise. A model of signal-dependent noise must accurately describe its properties to correctly account for the effect of noise. It should also be noted that studies must be carried out for images of different complexity to understand both positive and negative outcomes.

2.1. Noise models

White Gaussian noise is usually assumed to be additive, zero-mean, independent and identically distributed (i.i.d.) [35]. Under these assumptions, the resulting image z is modelled as follows:

$$z(x) = y(x) + \eta(x), \tag{1}$$

where y is a deterministic, noiseless image, $x \in \Omega \subset \mathbb{Z}^2$ is a pixel coordinate, and $\eta(x)$ is a random variable that follows the normal distribution $N(0, \sigma^2)$ with zero mean and variance σ^2.

Each x-coordinate corresponds to an independent realized value of the random variable $\eta(x)$, and together they form an additive white Gaussian noise (AWGN) field that distorts the y-image.

The Gaussian noise was generated using the random_noise function from the skimage.util module with a fixed random seed (92) to ensure reproducibility. The variance was set to $\sigma^2 = 25$ unless otherwise specified.

Poisson noise describes the random fluctuations that occur when discrete events, such as photons in medical images, are counted. It is a signal-dependent noise, meaning that its variance (spread of values) is proportional to the signal's mean value. This means that the more intense the image (higher the signal level), the greater the noise [32].

For large values of the mean (μ), the Poisson distribution is well approximated by a normal distribution with the same mean and variance:

$$P(\mu) \approx N(\mu, \mu), \tag{2}$$

where N is a normal distribution with expectation μ.

Equation (2) is based on a standard approximation in which a normal distribution approximates the Poisson distribution when the expected number of events is sufficiently large. This assumption is reasonable for typical pixel intensities in medical imaging when the mean photon count exceeds approximately 10–12, as shown in [36, 37]. Although a rigorous derivation of the optimality conditions is beyond the scope of this study, the use of this approximation allows for analytical tractability and prac-

ISSN 1814-4225 (print)
ISSN 2663-2012 (online)

tical relevance in moderate- to high-intensity imaging regimes.

In [32], the authors provide an intuitive justification for this approximation, which is based on the central limit theorem (CLT) and the Poisson distribution's closed property when adding random variables.

When modeling Poisson noise, special functions in software tools and approximation by Gaussian noise can be used, where the variance is equal to the value of the image pixel. This approach is valid for 8-bit images and is generally considered adequate when the pixel values exceed 10–15, as recommended in prior studies.

This approximation allows replacing the Poisson distribution family with a Gaussian distribution family with a non-constant (spatially varying) variance that depends on the pixel brightness. This simplifies the analysis and processing. In our experiments, the tested images predominantly featured medium- to high-intensity values, where the Gaussian approximation to Poisson noise remains valid.

The same set of images was used across all simulations, and each noise realization was regenerated for every trial using a fixed seed (0) to ensure consistency across methods.

2.2. Image model

Medical imaging encompasses various methods for obtaining images of a human body by processing biomedical signals. The resulting images differ depending on the imaging method and the study object, which affects their characteristics.

The effectiveness of compression methods largely depends on the image characteristics, including its complexity and the presence of noise. Therefore, the selection of test images is an important stage of the study. Visual information with a simpler structure is easier to compress without significant loss, whereas complex images are the opposite.

We used 10 images (med1.png - med10.png) obtained from the website [radiopaedia.org]. These are medical images with atypical diagnoses. To simulate the conditions under interest, the images were artificially noised according to the aforementioned noise models.

Fig. 1 shows an example of a wrist image: (a) original, (b) version with additive Gaussian noise intensity, (c) version with Poisson noise. Both noises are more noticeable in bright areas and almost invisible in dark areas.

2.3. Techniques for Controlling the Efficiency of Lossy Compression

When working with noisy images, one of the features of lossy compression is the ability to suppress noise, provided that the control parameters are properly tuned,

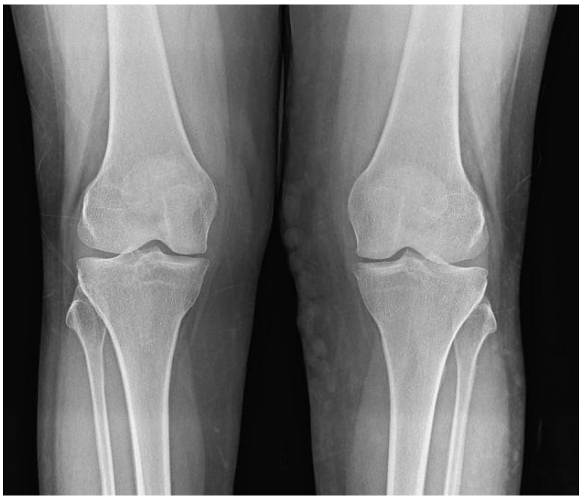

a

b

c

Fig. 1. Example of original (a), AWGN noisy (σ^2 =25) (b) and Poisson noisy (c) images

which allows compression to be performed near the OOP. Classical quality criteria are used to evaluate the effectiveness of compression, in particular MSE, as well as metrics related to visual perception, such as PSNR-HVS-M and MSSIM. These indicators involve comparing the decompressed noisy image I_{dec} with the original, noisy image I_{orig} for a set of artificially noised test images.

The main goal of lossy compression is to achieve an acceptable level of image quality at a maximum compression ratio (CR). Therefore, finding a balance between CR and quality is important, as an increase in CR inevitably leads to greater introduced distortions. The corresponding rate/distortion curves (RDCs) behave in a traditional manner, i.e., are monotonous with metric values worsening as CR increases.

If lossy compression is applied to a noisy image, the introduced distortions can be associated with both noise reduction and blurring of edges, details, or textures. All coders considered below are based on orthogonal transform (namely, DCT) performed in blocks (of different sizes). Distortions are introduced due to DCT coefficient quantization. Then, if the obtained DCT coefficients are small compared to the quantization step (QS) and most likely correspond to noise, they are assigned zero values, and the positive effect of noise removal occurs. This positive effect increases (till a certain moment) if the QS increases. In turn, if a DCT coefficient is larger and is not zeroed after quantization, this coefficient probably relates to information content. Then, undesired distortions are introduced, and their intensity increases if the QS increases. This means that optimum might be associated with the optimal operation point (OOP) and a certain QS or a parameter controlling compression (PCC) that is connected with the actual QS.

In practice, if OOP exists, there are two reasons for its compression. First, CR is OOP is usually quite large (see data in next Sections). Second, the quality of the image compressed in OOP is better than that of the uncompressed (original noisy) image. Meanwhile, to perform lossy compression of the noisy image in OOP, one must be sure that OOP exists and that PCC can be correctly set in OOP.

Despite the abovementioned verbal explanation of the effects occurring in the lossy compression of noisy images, the analytical statement and solving of the optimization task are problematic. The main problem deals with limited a priori information on the statistics of DCT coefficients for image content and noise components for a given image to be compressed. Then, one must rely on the numerical simulation data obtained for a set of typical images and noise characteristics. A special analysis is required where RDCs can be obtained by "comparing" the true image (without noise) to the compressed (originally noisy) image for different compression parameter values.

We are more interested in dependences that can only be obtained through simulation.

Having a compressed image $I^{c}_{ij}, i=1,...,I, j=1,...,J$, it is easy to calculate

$$MSE_{tc}=\frac{1}{IJ}\sum_{i=1}^{I}\sum_{j=1}^{J}(I^{tr}_{ij}-I^{c}_{ij})^{2}, \qquad (3)$$

where I^{tr}_{ij}, I^{c}_{ij} - pixel brightness value of true and compressed images, respectively; $I\times J$ - image size, and

$$PSNR_{tc}=10\log_{10}(\frac{255^{2}}{MSE_{tc}}). \qquad (4)$$

Other metrics can be similarly calculated using compressed noisy and true images.

In fact, to determine OOP or optimal CR, we need to establish whether an RDC have an extremum. The coordinate of the global minimum of the MSE_{tc} or the maximum of the $PSNR_{tc}$ is OOP in the traditional sense. It is also worth characterizing compression in OOP by the compression ratio CR_{OOP}, since this parameter is also important in practice.

In addition to traditional metrics, such as MSE and PSNR, visual quality metrics are widely applied in image compression. The PSNR-HVS-M metric [38] considers the peculiarities of the human visual system and is based on the discrete cosine transform (DCT). Its values are measured in decibels: the higher the value, the higher the visual quality. The MSSIM metric [39] is based on a wavelet transform and has a value ranging from 0 (very poor quality) to 1 (excellent quality).

Below, we have denoted PCCs for all the considered coders as Q. However, different encoders use different PCC parameters that vary in different limits, where its increase corresponds to a larger CR. QS can be any positive value, but it is usually less than 100. For the BPG coder, the PCC is simply called Q, which can only be a non-negative integer with a maximal value of 51. The larger Q, the larger CR. In contrast, for HEIF and AVIF coders, the quality factor (QF) serves as Q (PCC), where the larger QF corresponds to the smaller CR. QF is integer from 1 to 100.

2.4. Considered compression methods

Four encoders are considered in this paper. Let us give more details concerning each of them.

AGU is a high-quality lossy image encoder based on 32x32 DCT to decompose images into frequency components and reduce data size. The use of modern

ISSN 1814-4225 (print)
ISSN 2663-2012 (online)

techniques for lossless coding of quantized DCT coefficients and in-built deblocking after decompression is a feature of AGU.

Better Portable Graphics (BPG) is an image format developed by Fabrice Bellard in 2014 that is based on the HEVC (H.265) standard and provides high compression while maintaining quality. Block processing, pixel prediction, two-dimensional DCT, and adaptive quantization are used to extract and compress important details efficiently. Entropy coding is the final step, which further reduces the amount of data.

AVIF is a modern image format based on the AV1 video codec that delivers high quality with significant compression. It supports both lossy and lossless compression, 12-bit color depth, high-resolution (HDR), transparency, and metadata preservation. Thanks to the efficient AV1 coding algorithms, AVIF files can be 50-60% smaller than JPEGs with similar quality. The format is supported by leading browsers and popular graphical editors.

HEIF is a modern image format based on the HEVC (H.265) video codec that delivers high quality with a significant reduction in file size (up to 50-60% smaller than JPEG). The format supports 16-bit color depth, transparency, HDR and animation, making it suitable for professional graphics work. HEIF is especially popular on Apple devices.

Since Q for the BPG, AGU, AVIF and HEIF encoders has different meanings, the plots are given separately for each encoder (see examples in Fig. 2-7).

2.5. Software Configuration and Tools

All simulations were performed within a well-defined software environment to ensure the reproducibility of experiments.

The BPG codec (version 0.9.8) was executed using the command-line tools bpgenc.exe and bpgdec.exe [32].

The AGU encoder was executed via AGU.EXE, obtained from [33]; however, the developer provided no explicit version number.

The AVIF and HEIF codecs were used through the libheif library (version 1.19.7), which was integrated into the Python environment using the pillow_heif package (version 0.22.0) [34].

The simulations were conducted using Python 3.10.12, with the following key packages: OpenCV 4.8.0.76, NumPy 1.26.4, scikit-image 0.22.0, pandas 2.2.2, scikit-learn 1.5.0, sewar 0.4.5, psnrhvsm (custom ITU-T J.341 implementation)

All experiments were executed on a machine with an Intel Core i5-1335U CPU, 16 GB RAM, and Windows 11 x64 Pro.

3. Results and Discussion

3.1. Results obtained

We begin our analysis with the usual MSE_{tc} metric (3). In Fig. 2a - 2d, the data obtained for test medical images contaminated by AWGN with variance 25 for each encoder under study.

As shown in Fig. 2, MSE_{tc} varies in a wide range and behaves differently for different encoders. For the BPG encoder, at small Q (<23), MSE_{tc} for the given images remains almost the same. A further increase in Q leads to a decrease in the vicinity of the OOP for all 10 images in Fig. 2 a. Partial noise suppression is observed, characterized by a decrease in MSE_{tc}. Then, as Q increases further, MSE_{tc} steadily increases if Q becomes larger. Note that for all images, Q_{OOP} is practically the same and equal to 31, which agrees with the data in [21, 22].

For the AGU encoder, the MSE_{tc} dependences (Fig. 2,b) have values approximately equal to σ^2 for very small Q, they slowly increase till Q≈8, then they decrease till Q ≈20, having Q_{OOP}≈20=4σ, and, after this, start to increase again. Notably, there is no clearly defined minimum in the dependence of MSE_{tc} on Q for only one medical image (med9.png), which is the most complex.

Recall that for HEIF and AVIF, a large Q corresponds to a small CR. In the case of the AVIF encoder (Fig. 2,c), there are minima (OOPs) for Q about 45 for almost all tested images. The behavior of the HEIF encoder is similar to that of the AVIF encoder, but minima (OOPs) are observed for Q ≈ 35.

Fig. 3 shows the MSE_{tc} dependence for the test images with Poisson noise. The behavior of the dependence is similar to that of additive Gaussian noise.

AGU is the only encoder that does not have OOPs for all images with Poisson noise. For other encoders, the minimum MSE_{tc} is observed for all plots, but it is shifted to the side of higher Q values compared to OOPs for additive Gaussian noise with σ^2 =25. Tables 1 and 2 show the average OOP positions for all encoders.

For the BPG encoder, OOPs are observed for all test images, and Q_{OOP} is larger if the image mean I_{mean} is larger (image mean is approximately equal to $MSE_{tc}(Q=1)$). Q_{OOP} is approximately 38. For the AGU encoder, minima are observed for $Q_{OOP}≈4(MSE_{tc}(Q=1))^{0.5}=4(I_{mean})^{0.5}$. For AVIF, Q_{OOP} varies in rather wide limits from 24 to 36, with the main tendency of Q_{OOP} decreasing if MSE_{tc} (Q=100) increases. A similar tendency is observed for HEIF, but the range of Q_{OOP} variation is from 20 to 30. This means that, for AVIF and HEIF, additional studies are needed to propose automatic and accurate algorithms of optimal PCC setting in OOP.

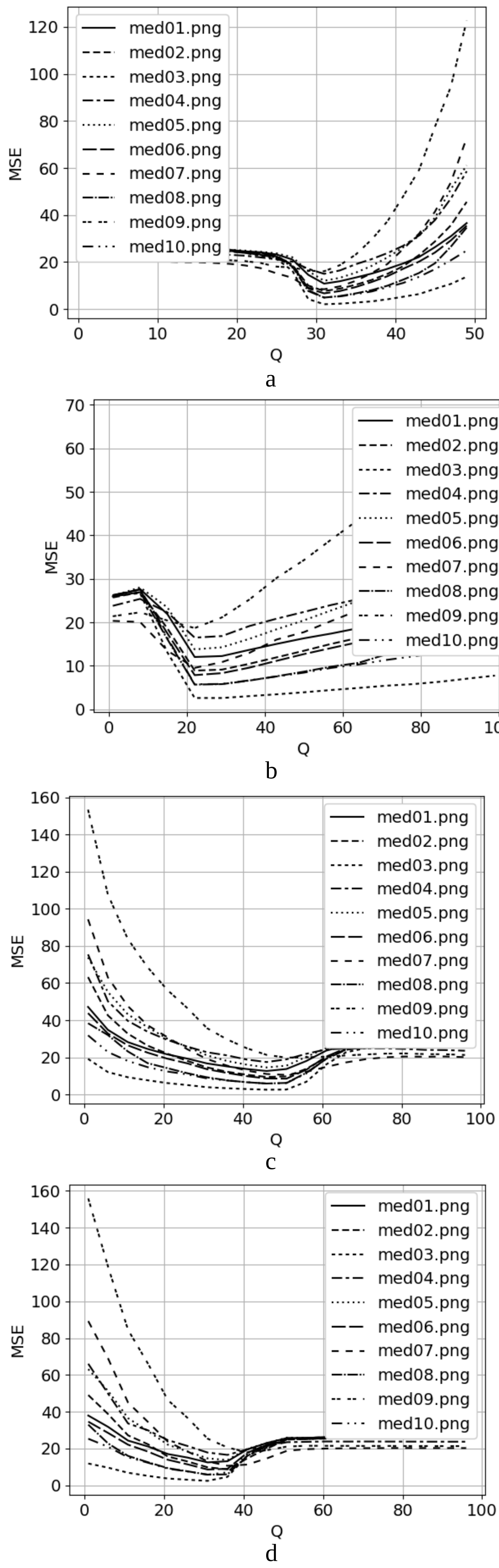

Fig. 2. Dependences of MSE_{tc} on Q for the AWGN noisy test images compressed by (a) – BPG, (b) – AGU, (c) – AVIF, (d) – HEIF

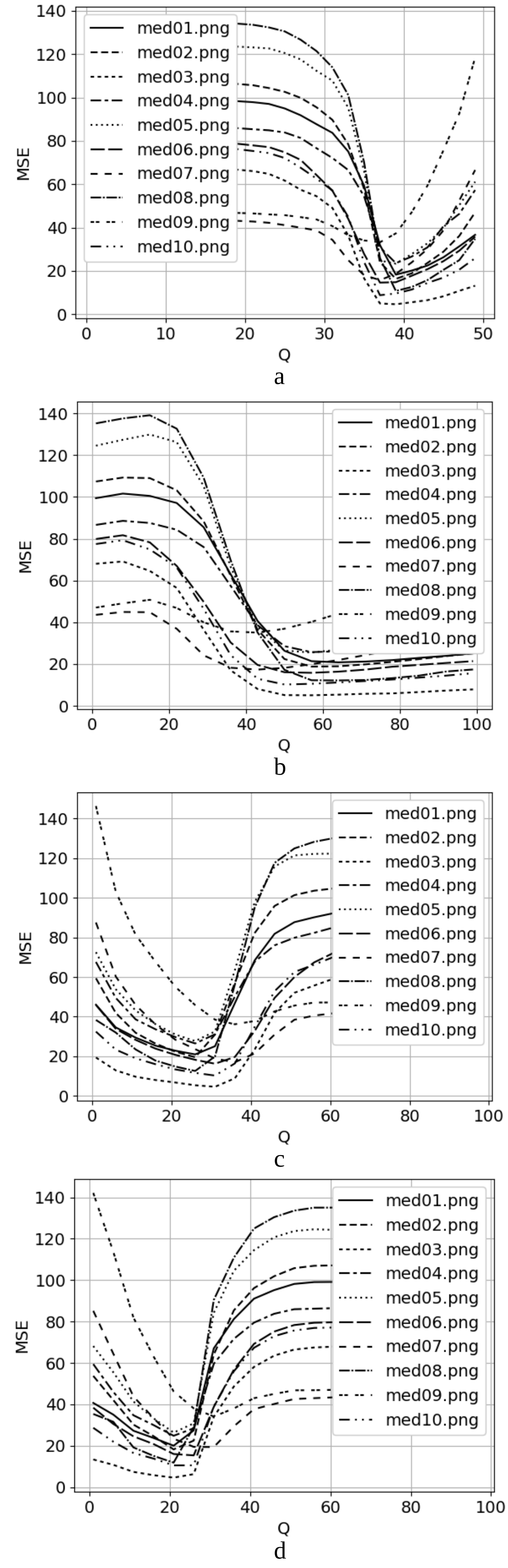

Fig. 3. Dependences of MSE_{tc} on Q for the Poison noisy test images compressed by (a) – BPG, (b) – AGU, (c) – AVIF, (d) – HEIF

ISSN 1814-4225 (print)
ISSN 2663-2012 (online)

According to the $PSNR_{tc}$ metric (Fig. 4, 5), the coordinates of the maxima coincide with the corresponding coordinates of the minima of the MSE_{tc} metric because these metrics are mutually dependent. The most interesting observations are as follows. First, for AWGN (Fig. 4), the BPG coder provides $PSNR_{OOP}$ in the limits from 36 to 45 dB, AGU coder – in the limits from 35.5 to 44 dB, AVIF – in the limits from 35 to 44 dB, and HEIF – in the limits from 35.5 to 44 dB. Therefore, the best results are provided by the BPG encoder and the worst – by the AVIF encoder although the difference is not large. Second, for Poisson noise (Fig. 5), the BPG coder produces $PSNR_{OOP}$ in the limits from 33 to 41.5 dB, AGU coder – in the limits from 32.5 to 41 dB, AVIF – in the range from 32.4 to 41 dB, and HEIF – in the range from 33 to 41.5 dB. Thus, the best results are again provided by the BPG encoder and the worst – by the AVIF encoder although the difference is not large again.

Since the compressed medical images are subject to visualization, considering the visual quality metric, MSSIM, is worth considering in our case.

Analysis shows that, according to the $MSSIM_{tc}$ metric (Fig. 6, 7), OOPs are observed as well and this happens for all ten test images in both Figures. Notably, the maxima's coordinates for a given image and a given coder almost coincide with the corresponding minima's coordinates of the MSE_{tc} metric. This means that optimizing compression according to MSE_{tc}, one simultaneously optimizes the visual quality of compressed images according to the visual quality metric $MSSIM_{tc}$ (in fact, the same holds for the metric PSNR-HVS-M_{tc}). Then, the recommendations for setting Q_{OOP} for the BPG and AGU encoders are the same as those in the previous section. Concerning the AVIF and HEIF encoders, Q_{OOP} for them vary in certain limits. For AWGN with a noise variance of 25 (Figures 6,c and 6,d), Q_{OOP} varies from 44 to 50 for AVIF and from 30 to 40 for HEIF. For Poisson noise (Figures 7,c and 7,d), Q_{OOP} varies from 26 to 34 for AVIF and from 20 to 32 for HEIF. Thus, additional research is needed to provide automatic and accurate procedures for optimal PCC setting in OOP for AVIF and HEIF. Comparison of $MSSIM_{tc}$ in OOPs shows that for a given test image and noise type, they are slightly better for the BPG encoder than for other considered compression techniques.

3.2. Statistical Analysis and Discussion

Finally, for better comparison, Tables 1 and 2 present the data after averaging (for the considered test images) for AWGN and Poisson noise cases, respectively. These are the average values (and standard deviations in some cases) for Q_{OOP}, quality metrics, and CR in OOP. CR in OOP is important because memory savings can be valuable if many images are acquired in some clinic and

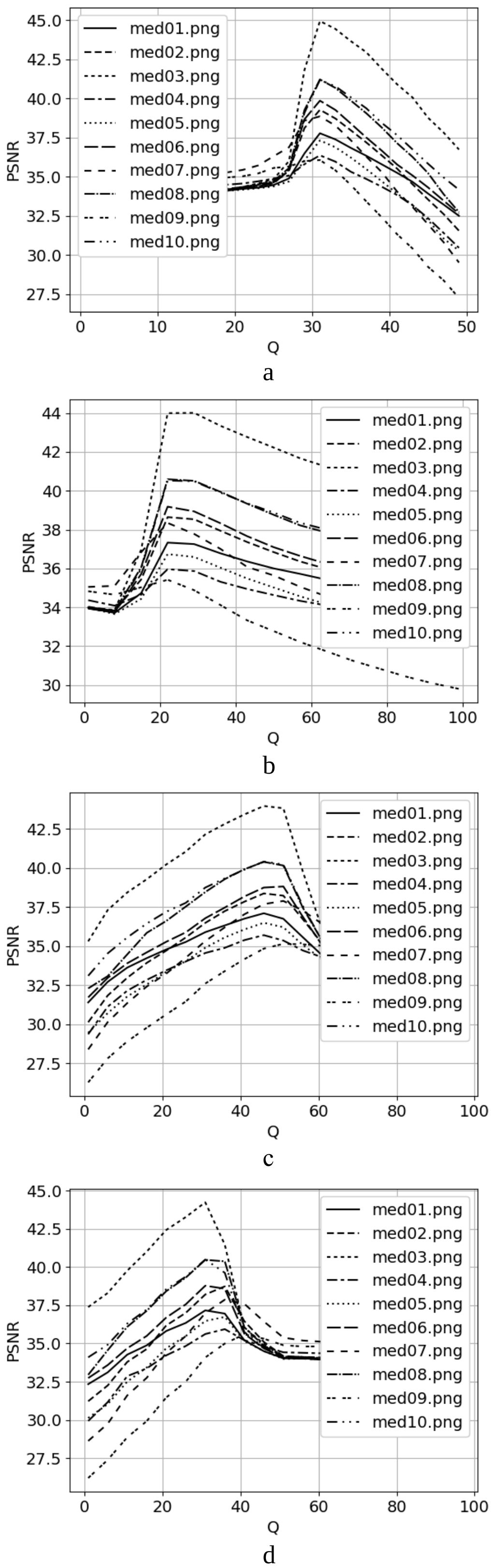

Fig. 4. Dependences of $PSNR_{tc}$ metric values on Q for the AWGN noisy test images compressed by (a) – BPG, (b) – AGU, (c) – AVIF, (d) – HEIF.

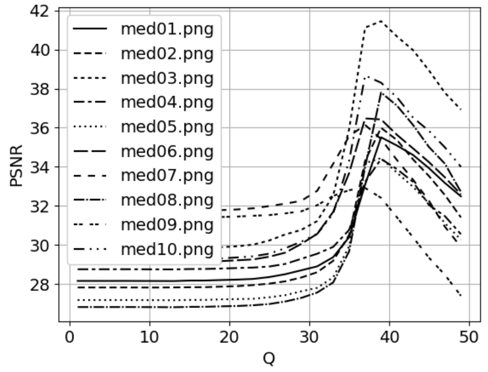

a

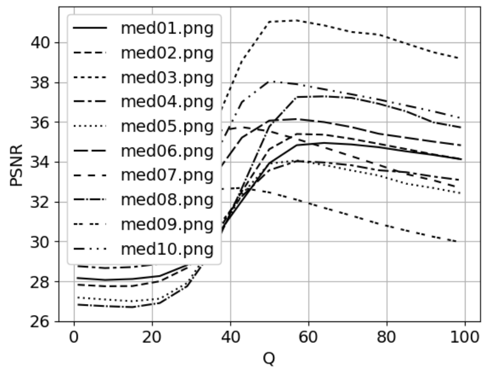

b

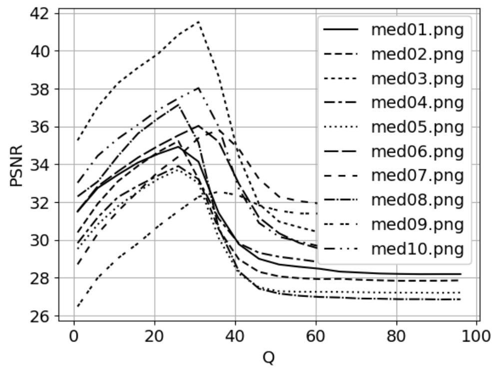

c

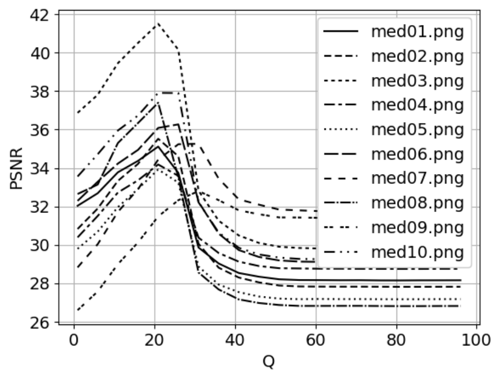

d

Fig. 5. Dependences of $PSNR_{tc}$ metric values on Q for the Poison noisy test images compressed by (a) – BPG, (b) – AGU, (c) – AVIF, (d) – HEIF.

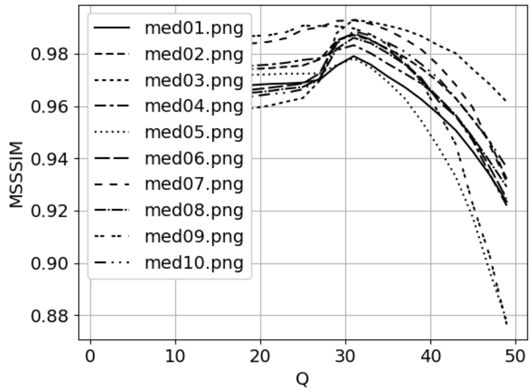

a

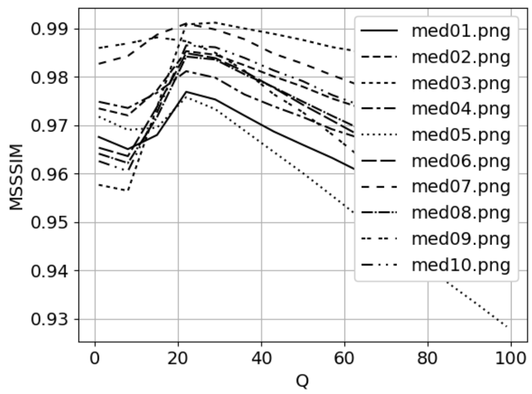

b

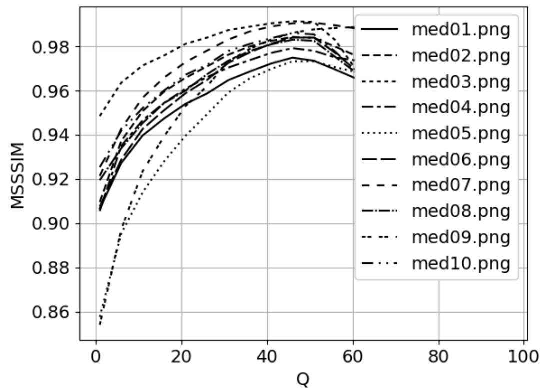

c

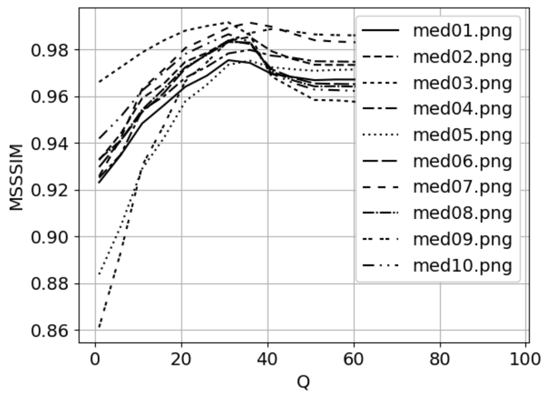

d

Fig. 6. Dependences of $MSSIM_{tc}$ on Q for the AWGN noisy test images compressed by (a) - BPG, (b) – AGU, (c) – AVIF, (d) - HEIF.

ISSN 1814-4225 (print)
ISSN 2663-2012 (online)

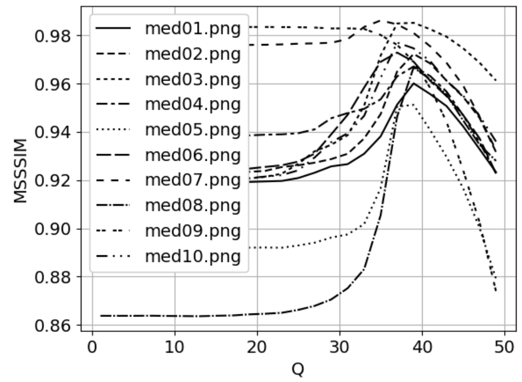

a

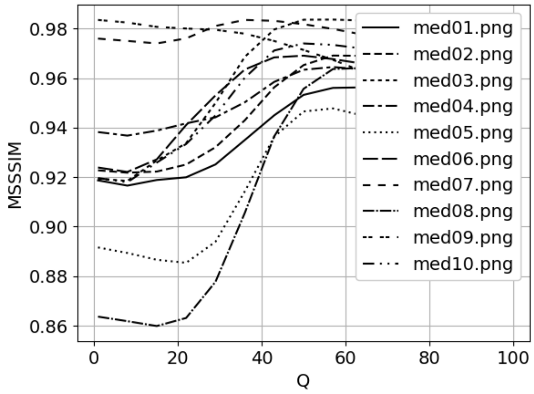

b

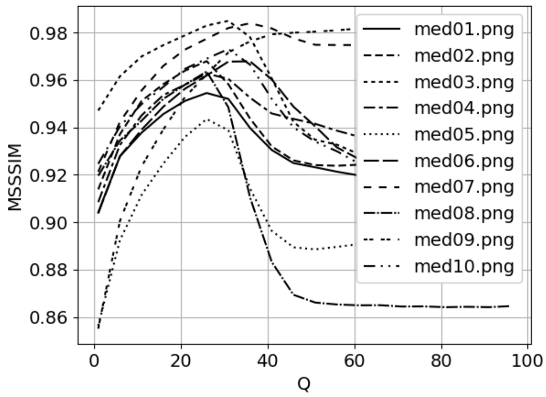

c

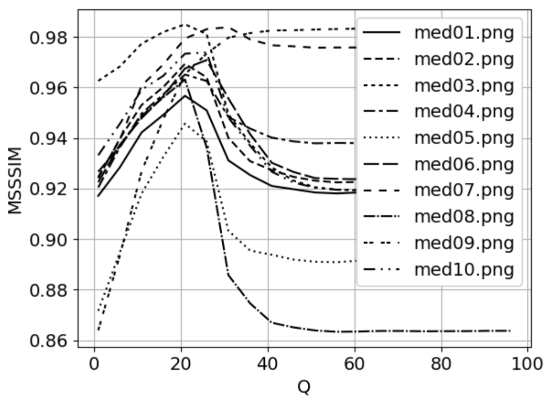

d

Fig. 7. Dependences of $MSSSIM_{tc}$ on Q for the Poison noisy test images compressed by (a) - BPG, (b) – AGU, (c) – AVIF, (d) - HEIF.

then saved. The mean CR values reach tens for AWGN and can even exceed 100 for Poisson noise. This means that memory savings can be very significant. In this sense, the results for the AGU encoder are the worst. Regarding the quality metrics in OOP, the BPG coder provides the best values of average MSE, PSNR, PSNR-HVS-M, and MSSIM. The worst results are produced by AVIF, but the difference is small. Thus, the BPG encoder appears to be the best practical solution.

To address concerns regarding the rigor of our statistical evaluation, we performed formal statistical significance tests and extended the analysis beyond reporting only average values and standard deviations. We applied one-way ANOVA (Analysis of Variance) tests to compare the performance of different codecs across five key metrics: MSE, PSNR, PSNR-HVS-M, compression ratio (CR), and MSSSIM.

ANOVA is a widely used statistical method that assesses whether the means of three or more groups (in our case, different codecs) differ significantly. It does so by analyzing the variance between groups compared with the variance within groups. A significant ANOVA result (indicated F-statistic and low p-value) suggests that at least one codec performs statistically differently from the others on the given metric.

The analysis was conducted on results aggregated over ten test images for each codec, separately for each noise condition (AWGN and Poisson noise). The findings demonstrate statistically significant differences among codecs for PSNR (AWGN: $F=42.39$, $p < 6.75\times10^{-27}$; Poisson: $F=99.99$, $p<4.48\times10^{-62}$), PSNR-HVS-M (AWGN: $F=29.28$, $p<1.09\times10^{-18}$; Poisson: $F=8.64$, $p<1.04\times10^{-5}$), CR (AWGN: $F=29.97$, $p<4.04\times10^{-19}$; Poisson: $F=14.37$, $p<2.64\times10^{-9}$), and MSSSIM (AWGN: $F=13.31$, $p<1.22\times10^{-8}$; Poisson: $F=27.59$, $p<1.25\times10^{-17}$). Although the differences in MSE were less pronounced and did not reach statistical significance for Poisson noise ($F=0.90$, $p=0.44$), they were significant for AWGN ($F=26.84$, $p<3.71\times10^{-17}$). This overall pattern confirms that codec performances differ meaningfully for most evaluated metrics across noise types.

Furthermore, we complemented the statistical tests with a ranking-based analysis identifying how frequently each codec achieved the best or worst results per image and metric:

PSNR metric:

The best: BPG for all 10 images for both noise types;
The worst: AGU and AVIF most frequently;

PSNR-HVS-M:

The best: BPG leads (9/10 AWGN, 8/10 Poisson);
The worst: AVIF and AGU dominate the worst rankings.

MSSSIM:

The best: BPG for all 10 images for both noise models;
The worst: AVIF and AGU evenly split poor rankings.

Table 1

The statistics for OOP for images contaminated by AWGN with variance 25

Coder	Average Q_{oop}	Average MSE ± std	Average PSNR ± std	Average PSNR-HVS-M ± std	Average CR	Average MSSIM ± std
AGU	24	9.92± 8.03	38.78± 4.35	37.14± 2.20	40.59	0.984± 0.007
AVIF	49	10.70± 8.55	38.47± 4.44	36.92± 2.51	52.35	0.984± 0.009
BPG	31	8.83± 6.86	39.31± 4.40	38.13± 2.37	48.09	0.987± 0.007
HEIF	35	10.07± 7.73	38.71± 4.32	37.25± 2.40	52.00	0.984 ± 0.008

Table 2

The statistics for OOP for images contaminated by Poisson noise

Coder	Average Qoop	Average MSE ± std	Average PSNR ± std	Average PSNR-HVS-M ± std	Average CR	Average MSSIM ± std
AGU	53	18.55± 14.94	35.97± 4.24	33.02± 2.83	98.46	0.968 ± 0.018
AVIF	31	18.93± 15.78	35.93± 4.49	32.94± 3.10	115.70	0.968± 0.020
BPG	38	16.81± 14.53	36.45± 4.51	33.61± 2.89	140.58	0.971± 0.017
HEIF	24	18.12± 14.72	36.09± 4.37	33.19± 3.00	110.16	0.969± 0.019

This comprehensive analysis confirms that BPG consistently delivers superior PSNR, perceptual quality (PSNR-HVS-M and MSSSIM), and competitive compression efficiency.

We provide robust evidence substantiating the superiority and trade-offs among codecs by combining formal hypothesis testing with per-image ranking statistics, strengthening the credibility of our conclusions.

4. Conclusions

This study performed a comprehensive comparison of four modern encoders (BPG, AGU, AVIF, HEIF) for compressing Gaussian or Poisson noise-contaminated medical images. In accordance with the task set, the following results were obtained:

- It is found that the MSEtc, PSNRtc and MSSIMtc metrics effectively identify the optimal operating points for the compression parameter (Q_{OOP}), at which the best ratio between image quality and compression ratio (CR) is achieved. For example, for AWGN noise, the BPG encoder achieves Q_{OOP}<≈ 31, average PSNR ≈ 39.31 dB, MSSIM ≈ 0.987, and CR ≈ 48.09. For Poisson noise, Q_{OOP} ≈ 38, PSNR ≈ 36.45 dB, MSSIM ≈ 0.971, and CR ≈ 140.58.
- It is shown that the BPG coder provides the best results for all studied metrics for both Gaussian and Poisson noise, demonstrating high image quality with a significant reduction in file size. By comparison, the AVIF encoder gives average PSNR ≈ 38.47 dB and MSSIM ≈ 0.984 with CR ≈ 52.35 for AWGN, and PSNR ≈ 35.93 dB, MSSIM ≈ 0.968 with CR ≈ 115.70 for Poisson noise.
- The AGU encoder was more effective for images with Gaussian noise, providing optimal Q_{OOP} values according to the theoretical model, with Q_{OOP} ≈ 24, PSNR ≈ 38.78 dB, MSSIM ≈ 0.984 and CR ≈ 40.59. However, it was less suitable for processing images with Poisson noise, where Q_{OOP} ≈ 53, PSNR ≈ 35.97 dB, MSSIM ≈ 0.968 and CR ≈ 98.46.
- For AVIF and HEIF encoders, significant variability in the position of the optimal Q_{OOP} operating point was found, e.g., for HEIF under Poisson noise Q_{OOP} varies around 24 with PSNR ≈ 36.09 dB, MSSIM ≈ 0.969 and CR ≈ 110.16, which complicates the automatic tuning of compression parameters. This indicates the need for further research on the stability and predictability of their characteristics. It is also desirable to develop practical algorithms for setting quality factors for these coders depending on noise type and intensity.
- It was found that compression at Q_{OOP} points allows not only to effectively reduce the size of images, but also to partially suppress noise without significant loss of diagnostically important information.

The obtained results have practical significance for medical image storage and transmission systems, particularly in telemedicine. Further studies should be combined with expert assessment by physicians to confirm the clinical suitability of the processed images.

Contributions of authors: conceptualization, methodology – **Volodymyr Lukin;** formulation of tasks, analysis **– Volodymyr Lukin, Viktoriia Naumenko;** development of model, software, verification **– Vitalii Naumenko;** analysis of results, visualization **– Mykyta Solodovnyk;** writing – original draft preparation **– Viktoriia Naumenko**, writing – review and editing **– Nadiia Kozhemiakina.**

Conflict of Interest

The authors declare that they have no conflict of interest concerning this research, whether financial, personal, authorship or otherwise, that could affect the research and its results presented in this paper.

ISSN 1814-4225 (print)
ISSN 2663-2012 (online)

Financing

This study was conducted without financial support.

Data Availability

The work has associated data in the data repository.

Use of Artificial Intelligence

The authors confirm that they did not use artificial intelligence methods while creating the presented work.

All the authors have read and agreed to the published version of this manuscript.

References

1. Kim, M. E., Ramadass, K., Gao, C., Kanakaraj, P., Newlin, N., Rudravaram, G., Schilling, K. G., Dewey, B., Archer, D., Hohman, T. J., Li, Z., Bao, S., Landman, B. A., & Khairi, N. M. Scalable, reproducible, and cost-effective processing of large-scale medical imaging datasets. *Imaging Informatics*, San Diego, United States, 16–21 February 2025. SPIE, 2025. 23 p. DOI: 10.48550/ARXIV.2408.14611.

2. Sachenko, A., Yatskiv, V., Sieck, J., & Su, J. Image Transmission in WMSN Based on Residue Number System. *International Journal of Computing,* 2024, vol. 23, iss. 1, pp. 126–133. DOI: 10.47839/ijc.23.1.3444.

3. Yatskiv, V., Sachenko, A., Yatskiv, N., Bykovyy, P., & Segin, A. Compression and Transfer of Images in Wireless Sensor Networks Using the Transformation of Residue Number System. *2019 10th IEEE International Conference on Intelligent Data Acquisition and Advanced Computing Systems: Technology and Applications (IDAACS),* Metz, France, 2019, pp. 1111–1114. DOI: 10.1109/IDAACS.2019.8924372.

4. Gopal, N., Kala, L., & Arun, L. Review on medical image compression. *International Journal of Advanced Research in Science, Communication and Technology*, 2023, pp. 54–64. DOI: 10.48175/ijarsct-12010.

5. Abduljaleel, I. Q., & Khaleel, A. H. Significant medical image compression techniques: a review. *TELKOMNIKA (Telecommunication Computing Electronics and Control)*, 2021, vol. 19, iss. 5, article no. 1612. DOI: 10.12928/telkomnika.v19i5.18767.

6. Singh, M., Kumar, S., Singh, S., & Shrivastava, M. Various image compression techniques: lossy and lossless. *International Journal of Computer Applications*, 2016, vol. 142, iss. 6, pp. 23–26. DOI: 10.5120/ijca2016909829.

7. Rojas-Hernández, R., Díaz-de-León Santiago, J. L., Barceló-Alonso, G., Bautista-López, J., Trujillo-Mora, V., & Salgado-Ramírez, J. C. Lossless medical image compression by using difference transform. *Entropy*, 2022, vol. 24, iss. 7, article no. 951. DOI: 10.3390/e24070951.

8. Kryvenko, L., Krylova, O., Lukin, V., & Kryvenko, S. Intelligent visually lossless compression of dental images. *Advanced Optical Technologies*, 2024, article no. 13. DOI: 10.3389/aot.2024.1306142.

9. Kumar, S. N., Haridhas, A. K., Lenin Fred, A., & Sebastin Varghese, P. Analysis of lossy and lossless compression algorithms for computed tomography medical images based on bat and simulated annealing optimization techniques. In: *Computational Intelligence Methods for Super-Resolution in Image Processing Applications*. Cham: Springer International Publishing, 2021, pp. 99–133. DOI: 10.1007/978-3-030-67921-7_6.

10. Elsayed, H. A., Majeed, Q. E., & Sherbiny, M. M. E. Non-decimated wavelet transform and vector quantization for lossy medical images compression. *Journal of Computer Science*, 2023, vol. 19, iss. 3, pp. 363–371. DOI: 10.3844/jcssp.2023.363.371.

11. Cavaro-Menard, C., Le Callet, P., Barba, D., & Tanguy, J.-Y. Quality assessment of lossy compressed medical images. In: *Compression of Biomedical Images and Signals*. London, UK: ISTE, 2008, pp. 101–128. DOI: 10.1002/9780470611159.ch5.

12. Sultana, Z., Nahar, L., Tasnim, F., Hossain, M. S. & Andersson, K. Lossy compression effect on color and texture based image retrieval performance. In: *Intelligent Computing & Optimization*. Cham: Springer International Publishing, 2022, pp. 1159–1167. DOI: 10.1007/978-3-031-19958-5_108.

13. Kumar, D. V. The contemporary significance of image compression standards in medical imaging. *Futuristic Trends in Medical Sciences*, vol. 3, book 10. Iterative International Publisher, Selfypage Developers Pvt Ltd., 2024, pp. 138–163. DOI: 10.58532/v3bfms10p4ch3.

14. European Society of Radiology (ESR). Usability of irreversible image compression in radiological imaging: a position paper. *Insights into Imaging*, 2011, vol. 2, no. 2, pp. 103-115. DOI: 10.1007/s13244-011-0071-x.

15. Prasath, V. B. S. Quantum noise removal in X-ray images with adaptive total variation regularization. *Informatica*, 2017, vol. 28, no. 3, pp. 505–515. DOI: 10.15388/informatica.2017.141.

16. Rodrigues, I., Sanches, J., & Bioucas-Dias, J. Denoising of medical images corrupted by Poisson noise. *Proceedings of the 15th IEEE International Conference on Image Processing*, 12–15 October 2008, San Diego, CA, USA. IEEE, 2008. DOI: 10.1109/ICIP.2008.4712115.

17. Badgainya, S., Sahu, P. P., & Awasthi, P. V. Image denoising for AWGN corrupted image using OWT and thresholding. *International Journal of Trend in Scientific Research and Development*, 2018, vol. 2, no. 6, pp. 220–226. DOI: 10.31142/ijtsrd18338.

18. Kryvenko, S., & Lukin, V. Peculiarities of noisy image lossy compression. *Herald of Khmelnytskyi National University. Technical Sciences*, 2024, no. 333(2), pp. 278–283. DOI: 10.31891/2307-5732-2024-333-2-44.

19. Al-Shaykh, O. K., & Mersereau, R. M. Lossy compression of noisy images. *IEEE Transactions on Image Processing*, 1998, vol. 7, no. 12, pp. 1641–1652. DOI: 10.1109/83.730376.

20. Cheng, K. L., Xie, Y., & Chen, Q. Optimizing Image Compression via Joint Learning with Denoising. Lecture Notes in Computer Science, vol. 13679. Cham: Springer, 2022, pp. 56–73. DOI: 10.1007/978-3-031-19800-7_4.

21. Kovalenko, B., Lukin, V., Kryvenko, S., Naumenko, V., & Vozel, B. BPG-based automatic lossy compression of noisy images with the prediction of an optimal operation existence and its parameters. *Applied Sciences*, 2022, vol. 12, no. 15, article 7555. DOI: 10.3390/app12157555.

22. Kovalenko, B., Lukin, V., & Vozel, B. BPG-based lossy compression of three-channel noisy images with prediction of optimal operation existence and its parameters. *Remote Sensing*, 2023, vol. 15, no. 6, article 1669. DOI: 10.3390/rs15061669.

23. Bai, Y., Liu, X., Wang, K., Ji, X., Wu, X., & Gao, W. Deep Lossy Plus Residual Coding for Lossless and Near-lossless Image Compression. *IEEE Transactions on Pattern Analysis and Machine Intelligence*, 2024, vol. 46, no. 5, pp. 3577–3594. DOI: 10.1109/TPAMI.2023.3348486.

24.Makarichev, V., Lukin, V., & Brysina, I. Progressive DCT-based coder and its comparison to atomic function-based image lossy compression. *Proceedings of the 16th IEEE International Conference on Advanced Trends in Radioelectronics, Telecommunications and Computer Engineering (TCSET)*, 22–26 February 2022, Lviv-Slavske, Ukraine. IEEE, 2022. DOI: 10.1109/TCSET55632.2022.9766871.

25. Abramova, V., Kryvenko, S., Abramov, S., Makarichev, V., & Lukin, V. A fast procedure for image lossy compression by ADCTC using prediction of distortions' MSE. In: *Integrated Computer Technologies in Mechanical Engineering – 2022*. Cham: Springer Nature Switzerland, 2023, pp. 625–635. DOI: 10.1007/978-3-031-36201-9_52.

26. Mansuri, I., & Bhatt, M. Image encryption and compression using discrete wavelet transform and adaptive thresholding. *International Journal of Computer Science and Engineering*, 2016, vol. 3, no. 11, pp. 48–54. DOI: 10.14445/23488387/IJCSE-V3I11P110.

27. Shahnaz, R., Walkup, J. F., & Krile, T. F. Image compression in signal-dependent noise. *Applied Optics*, 1999, vol. 38, no. 26, article no. 5560. DOI: 10.1364/AO.38.005560.

28. Kovalenko, B., Lukin, V., Kryvenko, S., Naumenko, V., & Vozel, B. BPG-based automatic lossy compression of noisy images with the prediction of an optimal operation existence and its parameters. *Applied Sciences*, 2022, vol. 12, iss. 15, article no. 7555. DOI: 10.3390/app12157555.

29. Wang, Z., Bovik, A. C., & Sheikh, H. R. Structural similarity based image quality assessment. In: *Digital Video Image Quality and Perceptual Coding*. CRC Press, 2017, pp. 225–242. DOI: 10.1201/9781420027822-7.

30. Zhang, R., Isola, P., Efros, A. A., Shechtman, E., & Wang, O. The Unreasonable Effectiveness of Deep Features as a Perceptual Metric. *2018 IEEE/CVF Conference on Computer Vision and Pattern Recognition (CVPR), Salt Lake City*, UT, 18–23 June 2018, pp. 586–595. DOI: 10.1109/CVPR.2018.00068.

31. Rudnichenko, N., Vychuzhanin, V., Vychuzhanin, A., Bercov, Y., Levchenko, A., & Otradskya, T. Adaptive Digital Image Compression. In: Digital Economy, Business Analytics, and Big Data Analytics Applications. *Studies in Computational Intelligence*, vol. 1010. Cham: Springer, 2022, pp. 45–53. DOI: 10.1007/978-3-031-05258-3_5.

32. Bellard, F. *BPG image format*. Available at: https://bellard.org/bpg/ (accessed 30 March 2025).

33. Ponomarenko, N. *AGU image coder*. Available at: https://www.ponomarenko.info/agu.htm (accessed 30 March 2025).

34. Awxkee. *AVIF-Coder: Custom AVIF encoder for research and development*. Available at: https://github.com/awxkee/avif-coder (accessed 30 March 2025).

35. Azzari, L., Borges, L. R., & Foi, A. Modeling and estimation of signal-dependent and correlated noise. In: *Denoising of Photographic Images and Video*. Cham: Springer International Publishing, 2018, pp. 1–36. DOI: 10.1007/978-3-319-96029-6_1.

36. Chen, M.-J., & Bovik, A. C. Fast structural similarity index algorithm. *2005 IEEE International Conference on Acoustics, Speech, and Signal Processing (ICASSP)*, Philadelphia, PA, USA, 18–23 March 2005, vol. 2, pp. ii–998. DOI: 10.1109/ICASSP.2005.1449869.

37. *Statistics Online. Lesson 28: Inferences for Two Population Means*. Available at: https://online.stat.psu.edu/stat414/lesson/28/28.2 (accessed 19 March 2025)

38.Ponomarenko, N., Silvestri, F., Egiazarian, K., Carli, M., Astola, J., & Lukin, V. On between-coefficient contrast masking of DCT basis functions. *Proceedings of the Third International Workshop on Video Processing and Quality Metrics*, 2007, article 4.

39. Wang, Z., Bovik, A. C., Sheikh, H. R., & Simoncelli, E. P. Image quality assessment: from error visibility to structural similarity. *IEEE Transactions on Image Processing*, 2004, vol. 13, no. 4, pp. 600–612. DOI: 10.1109/TIP.2003.819861.

Received 14.03.2025, Accepted 20.05.2025

ISSN 1814-4225 (print)
ISSN 2663-2012 (online)

ПОРІВНЯЛЬНИЙ АНАЛІЗ ЕФЕКТИВНОСТІ МЕТОДІВ СТИСНЕННЯ BPG, AGU, AVIF ТА HEIF ДЛЯ МЕДИЧНИХ ЗОБРАЖЕНЬ, ПОШКОДЖЕНИХ ШУМАМИ ДВОХ ТИПІВ

В. В. Науменко, В. В. Лукін, В. М. Науменко,
Н. В. Кожемякіна, М. С. Солодовник

Предметом дослідження є стиснення з втратами за допомогою кодерів BPG, AGU, AVIF та HEIF медичних зображень з різним рівнем візуальної складності, спотворених адитивним гаусівським та пуассонівським шумом. **Метою** роботи є порівняння кодерів щодо оптимальних параметрів стиснення зображень та вибір найбільш придатної метрики для визначення оптимальної робочої точки. Розглянуті **задачі** включають вибір тестових зображень у відтінках сірого 512x512 з різним ступенем візуальної складності, включаючи візуально складні зображення з великою кількістю країв та текстур, помірно складні зображення з краями та текстурами, що прилягають до однорідних областей, та візуально прості зображення, що складаються переважно з однорідних областей; встановлення метрик оцінки якості зображень та оцінка їх ефективності при різних параметрах стиснення кодерів; вибір однієї або декількох метрик, які чітко визначають положення оптимальної робочої точки; надання на основі отриманих результатів рекомендацій щодо стиснення медичних зображень, спотворених адитивними гаусівським та пуассонівським шумами, чотирма кодерами з метою максимального наближення якості відновленого зображення до зашумленого оригіналу. Використані **методи** включають методи оцінки якості зображень з використанням метрик MSE, PSNR і MSSIM, а також програмне моделювання на мові Python без використання вбудованого генератора пуассонівського шуму. **Результати** показують, що для всіх цих метрик можна визначити оптимальні робочі точки (OPT), коли якість стисненого зображення є кращою за якість відповідного зашумленого вихідного зображення при достатньо високому ступені стиснення. Більше того, досягнення відповідного балансу між ступенем стиснення та якістю зображення призводить до часткового зменшення шуму без помітного спотворення інформативності стисненого зображення. Дослідження підкреслює важливість використання відповідних метрик для оцінки якості стиснених медичних зображень і дає уявлення про визначення параметра стиснення Q для досягнення оптимальної робочої точки BPG-кодера для конкретних зображень. Однак положення OPT та її наявність залежать не тільки від складності зображення, але й від обраного кодера. **Висновки**. Наукова новизна отриманих результатів полягає в наступному: 1) розгляд моделей шуму та рівнів параметрів, характерних для медичних зображень, а саме: адитивного гаусівського шуму такої інтенсивності, що він приблизно відповідає ледь помітним відмінностям, та сигнально-залежного пуасонівського шуму; 2) Аналіз багатомасштабного індексу структурної подібності (MS-SSIM), який раніше не досліджувався в роботах зі стиснення зашумлених медичних зображень з втратами; 3) детальне дослідження кодерів AVIF та HEIF для визначення того, чи спостерігається для них оптимальна робоча точка (OPT) і за яких шумових умов; 4) використання набору даних, що складається з десяти медичних зображень різної візуальної складності, з узагальненими тенденціями, виявленими для різних структурних типів; 5) здатність багатьох метрик мати OPT для зображень помірної візуальної складності або зображень, в яких переважають однорідні ділянки; 6) для пуассонівського шуму дослідження підкреслює залежність Q в OPT від середньої інтенсивності зображення, яка може бути обґрунтовано розрахована для заданого зображення, призначеного для стиснення, на основі отриманих результатів; 7) Оскільки різні кодери використовують різні параметри, які керують стисненням, для різних кодерів потрібні різні підходи до визначення OPT; 8) Коефіцієнти стиснення для зображень, стиснутих в OPT, досить високі, що додатково обґрунтовує доцільність стиснення зображень в OPT або біля неї.

Ключові слова: стиснення зображення з втратами; BPG; AGU; AVIF; HEIF; AWGN; шум Пуассона; оптимальна робоча точка.

Науменко Вікторія Володимирівна – канд. техн. наук, доц. каф. інформаційно-комунікаційних технологій ім. О. О. Зеленського, Національний аерокосмічний університет «Харківський авіаційний інститут», Харків, Україна.

Лукін Володимир Васильович – д-р техн. наук, проф., зав. каф. інформаційно-комунікаційних технологій ім. О. О. Зеленського, Національний аерокосмічний університет «Харківський авіаційний інститут», Харків, Україна.

Науменко Віталій Миколайович – асп. каф. інформаційно-комунікаційних технологій ім. О. О. Зеленського, Національний аерокосмічний університет «Харківський авіаційний інститут», Харків, Україна.

Кожемякіна Надія Володимирівна – канд. техн. наук, доц. каф. інформаційно-комунікаційних технологій імені О. О. Зеленського, Національного аерокосмічного університету ім. М. Є. Жуковського «Харківський авіаційний інститут», Харків, Україна

Солодовник Микита Сергійович – асп. каф. інформаційно-комунікаційних технологій ім. О. О. Зеленського, Національний аерокосмічний університет «Харківський авіаційний інститут», Харків, Україна.

Viktoriia Naumenko – PhD of Technical Science, Associate Professor at the Department of Information-Communication Technologies named after O. O. Zelensky, National Aerospace University "Kharkiv Aviation Institute", Kharkiv, Ukraine,
e-mail: v.naumenko@khai.edu, ORCID: 0000-0002-5291-6032.

Volodymyr Lukin – Doctor of Technical Science, Professor, Head of the Department of Information-Communication Technologies named after O. O. Zelensky, National Aerospace University "Kharkiv Aviation Institute", Kharkiv, Ukraine,
e-mail: v.lukin@khai.edu, ORCID: 0000-0002-1443-9685.

Vitalii Naumenko – PhD Student of the Department of Information-Communication Technologies named after O. O. Zelensky, National Aerospace University "Kharkiv Aviation Institute", Kharkiv, Ukraine,
e-mail: v.m.naumenko@khai.edu, ORCID: 0009-0005-8426-6635.

Nadiia Kozhemiakina – PhD of Technical Science, Associate Professor at the Department of Information-Communication Technologies named after O. O. Zelensky, National Aerospace University "Kharkiv Aviation Institute", Kharkiv, Ukraine,
e-mail: n.kozhemiakina@khai.edu, ORCID: 0000-0001-8194-5847.

Mykyta Solodovnyk – PhD Student of the Department of Information-Communication Technologies named after O. O. Zelensky, National Aerospace University "Kharkiv Aviation Institute", Kharkiv, Ukraine,
e-mail: m.solodovnyk@itc.khai.edu, ORCID: 0009-0009-9889-3591.